

# SOME SPECIAL DYNAMIC PROBLEMS WITH AEROSPACE STRUCTURES<sup>1</sup>

Huba ÖRY

Institut für Leichtbau  
RWTH Aachen  
D-5100 Aachen, Wülnerstraße 7.  
Germany

Received: Nov. 10, 1992

## Abstract

After a short review of dynamic phenomena, identification and analyses concerning the aerospace structures, some general remedies will be discussed. In the second part of the lecture, some selected special problems and the corresponding solutions will be presented.

## 1. Introduction

Aerospace structures must be light, consequently they become flexible, thin-walled and susceptible to buckling and vibrations. In my short lecture, I would like to show some specific problems connected to the structural dynamics.

After a short review of the dynamic phenomena and their consequences, some problems specific to this engineering branch will be shown, with references to usual solutions.

Dynamic phenomena occur in the form of different excitations, transient, periodic or random, but also as self-excited or parametric vibrations, as summarized in *Table 1*.

In order to analyse these problems, the aerospace structure should be idealized by mathematical models. Especially for large number parametric and optimization studies, reduced DOF models are welcome. Among analysts, the combination of analytical and numerical methods now finds growing interest (*Table 2*).

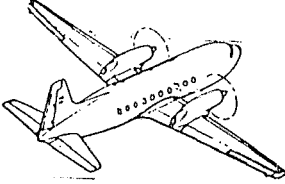
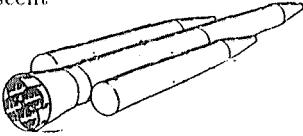
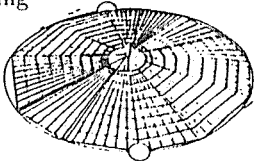
Similarly, dynamic response calculations should be rendered quick and interpreted easily, mainly for preliminary studies. *Table 3* summarizes different usual procedures with special reference to non-linearities.

Excessive dynamic responses jeopardize the correct function of the vehicle or lead to structural failure, as summarized in *Table 4*.

---

<sup>1</sup>Lecture held at the Technical University of Budapest, Institute of Vehicle Engineering, Nov. 9, 1992.

**Table 1**  
Dynamic Phenomena with Aerospace Structures

Dynamic phenomena	Aircraft 	Transportation systems and Spacecraft Ascent 	Orbiting 
Transients	Rolling on the airport Gust in the flight Manoeuver Landing Impacts (bird, stone, hail) Crash	Thrust building-up and decay Release for start staging, jettisoning Gusts Pyrotechnic shocks	Attitude control, thruster shocks shadow phases rendez-vous; docking meteorites and debris
Periodic excitations	Aircraft propeller Helicopter Rotor All turning machineries	Chugging (combustion instability) Pogo	Orbit frequency, shadow phase turning machineries
Random loads	Random gusts Buffeting Acoustics	Random gusts Buffeting Acoustics, Noises Structure born vibrations	Environment noises (inspace stations)
Parametric excitation		Combustion chamber vibrations	Release of a cable boom
Self excited vibrations	Lifting surface flutter (aerodynamic-mechanic couplings)	Pogo (thrust-feed-system- fluid-structure-coupling)	Thermal-mechanical couplings

**Table 2**  
Structure identification — Mathematical modelling

- Beam-like or regular structures, analytical methods
  - stiffness matrix
  - fluid-structure interaction
  - fluid compressibility
  - eigenmodes, modal calculation, damping concept
- Non-regular, or awkward structures, numerical methods
  - finite element method — stiffness matrix
  - mathematical model condensation
  - ... see above ...
- Hybrid procedures (numerical-cum-analytical methods)
- Effective mass concept
  - selection of significant eigenmodes
  - substructure coupling
- Experimental identification
  - in frequency domain
    - multi-point harmonic force excitation
    - single-point harmonic force excitation
    - base motion harmonic excitation
  - in time domain
    - analysing responses to transient excitation

**Table 3**  
Usual dynamic analyses with aerospace structures — Response calculations

- Modal synthesis
  - proportional damping — reduction to SDOF systems
  - linear systems only
  - for non-linear systems — iteration
- Physical coordinates, numerical integration of the DEQ
  - Newmark
  - Wilson, etc.
  - for linear and non-linear systems, but very time-consuming
- Physical coordinates, transfer matrices in the time domain
  - for linear and non-linear systems
  - (less time-consuming than numerical integration)
- Response calculation in the frequency-domain
  - Fourier transforms — transfer functions —
  - Fourier transforms
  - linear systems only (or iteration)

Guidance and control sensors can be seriously disturbed by vibration outputs. Large amplitudes hurt the clearance limits between substructures or block the control surfaces, or the gimbaling rocket nozzles.

**Table 4**  
Failure mechanisms due to dynamic response

- Sensor malfunction (guidance and control)
- Excessive deformation (clearance, blockage, control, malfunction)
- Structural collapse (instability, buckling, failure, leakage)
- Fatigue failure
- Failure of electronic components

The vibration velocity concept  
Stresses  $\Rightarrow$  vibration velocity

The most frequent troubles caused by dynamic responses are due to mechanical stresses, as structural collapse, rupture or fatigue, or also the failure of electronic devices, black-boxes and cables. Mechanical stresses are proportional to the vibrations velocity, therefore the velocity of vibrations is more suitable to judge the criticality of a dynamic output than the acceleration.

This statement will be explained in more details in §2.

Dynamic excitations cannot be avoided, therefore remedies have to be found in order to reduce the danger of the consequences. General methods cannot be applied, there are different devices and design rules for different sort of excitations, as summarized in the *Table 5*. More details will be explained in some specific cases in §3.

## 2. The Vibration-Velocity Concept

### *2.1 The Vibration Propagation in a Uniform Elastic Rod*

If the end of a uniform elastic rod will be hit by a force

$$P = \sigma A, \tag{1}$$

the stress will propagate with the velocity of the stress-wave  $c$ . After the time  $t$ , the length  $l = ct$  will be compressed by stress  $\sigma$  and, consequently, this length will be shortened by

$$\Delta l = \frac{\sigma}{E} l = \frac{\sigma}{E} ct \tag{2}$$

Table 5

How to reduce excessive dynamic responses? — Possible remedies, passives and actives

- Tuning: avoid highly excited frequencies (without approaching others)
- Damping (if applicable)
  - helps in harmonic resonance excitations
  - hardly helps in transients
  - is harmful in overcritical harmonic excitations
  - is rather harmful if substructures should be decoupled from an excited main body
  - is possibly harmful for self-excited phenomena
- Tuned dynamic vibration absorber
  - helps only in a narrow frequency band
  - and only in case of periodic resonance excitation
- Dynamic isolator (best known for helicopter rotor isolation)
  - helps in case of periodic excitation within a limited, but not very narrow frequency band
- Non-linearities (in stiffness and/or in damping)
- Active control
  - gust intensity reduction
  - flutter suppression
  - in-flight tuning
  - active damping force

giving an end velocity to the initial section of

$$V = \frac{\Delta l}{t} = \frac{\sigma}{E}c. \quad (3)$$

This reasoning enables us to define the stress in an elastic medium, if the vibration velocity is known

$$\sigma = E \frac{V}{c}. \quad (4)$$

The same argumentation shows that all the sections within the shadowed area of the rod, in *Fig. 1*, have velocity  $v$ . In this way the momentum-equation will define the stress-wave velocity as follows

$$\int P dt = m \Delta V, \quad (5)$$

$$A \sigma \Delta t = A c t \rho \frac{\sigma}{E} c, \quad (6)$$

$$c^2 = \frac{E}{\rho}, \quad (7)$$

$$c = \sqrt{\frac{E}{\rho}}. \quad (8)$$

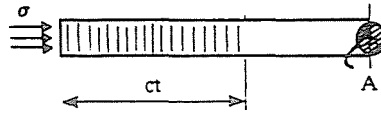


Fig. 1. Propagation of stress in a rod

The same analysis can be repeated on a modal basis. We consider a rod with the finite length of  $L$  which experiences a velocity shock with this velocity  $V_0$ , given by a very large rigid mass  $M$  arriving with velocity, as shown in Fig. 2. The relative velocity ( $-V_0$ ) can be developed in modal components and used as initial condition.

The absolute velocity will be subsequently defined at each instant as the sum of the local relative modal velocities and the transport velocity  $V_0$ .

In this chapter, we have found out that for a shock-excited rod the absolute vibration velocity measured at one specific point of the structure is directly proportional to the stress at the same location in the same direction if the propagation of the stress is due to an impact force applied.

## 2.2 The Relation between the Modal Velocity and the Modal Stress in a Free Vibration of a Continuous Beam

There exists a similar relation between the maximum stress and the maximum vibration velocity in the case of a pure free modal vibration as well:

$$\sigma_{max} = \kappa_i \sqrt{E \cdot \rho} \cdot V_i \quad (9)$$

$$= \kappa_i \sqrt{E \cdot \rho} \cdot (a_i \omega_i). \quad (10)$$

Here, however, the modal velocity  $v_i = a_i \omega_i$  and the modal stress  $\sigma_{max,i}$  are measured at different locations as shown in Fig. 3. For the formulas in Fig. 3, the beam is uniform and has a full rectangular cross-section. For other cross-section forms,

$$\kappa = \frac{1}{2} \cdot \frac{H}{r_g} \quad (11)$$

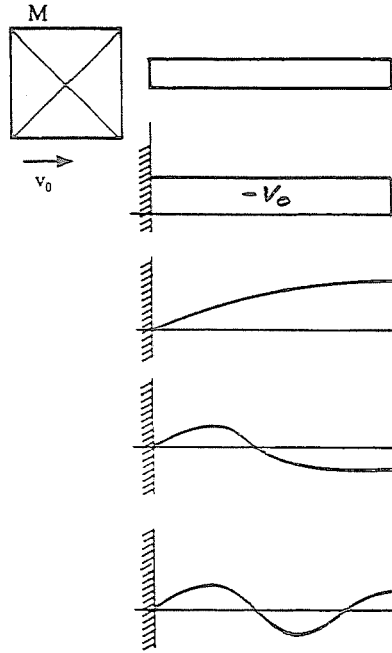


Fig. 2. Development of relative velocity in modal components

will hold, where  $H$  is the height and  $r_g$  — the radius of gyration of the cross section. This formula shows that  $\kappa$  is equal to 1.73, 2, 1 and 1.41 for a rectangular, circular, two-flange, and thin-walled tube cross-section forms, respectively. In all cases, only the bending or extensional flexibility (no shear) has been considered.

It is worth noting that for a simply supported beam with a concentrated central mass  $m$  ( $m/m$  beam = 10), we find  $\kappa = 9.7$ .

### 2.3 Correlation between Vibration Velocity and Stresses for Different Materials

The formula:

$$\sigma_i = \kappa \sqrt{E\rho} \cdot V_i \tag{12}$$

has been explained in chapter 2.1 and in Fig. 3. Factor  $\sqrt{E\rho}$  is dependent on the structural materials, as shown in Table 6.

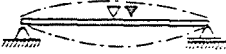
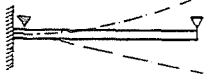
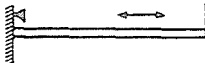
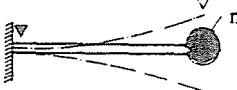
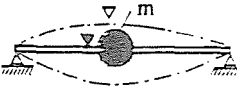
Actual Case	Proportionality: $\kappa$
	1,732
	1,732
	1
	$\sim 1,48 \sqrt{1 + 4,11 \frac{m}{m_{beam}}}$
	$\sim 2,12 \sqrt{1 + 2 \frac{m}{m_{beam}}}$

Fig. 3. Relation between the maximum modal vibration velocity and modal stress for uniform beams with full rectangular cross-section and without shear deformations.  
 Location of:  $\nabla$  modal displacement (velocity, acceleration) measurement;  $\nabla$  modal stress measurement

Consequently, a vibration velocity of e.g. 1 m/sec and  $\kappa = 1$  corresponds to a stress of  $1.45 \cdot 10^7 \text{ N/m}^2$  (or  $14.5 \text{ N/mm}^2$ ) in a light-alloy beam. We recall, however, to §2.1 where we stated that  $\kappa$  could be for a SDOF system easily as high as 10.

In general, in aerospace structures vibration velocities up to 1 - 2 m/sec are allowable, depending on the circumstance whether a unique stress peak or an alternating load has to be taken into account.



**Table 6**  
Factor  $\sqrt{E\rho}$  is dependent on the structural materials

Material	Velocity of shock propagation			
	$\rho$ kg/m <sup>3</sup>	$E$ Pa	$c = \sqrt{\frac{E}{\rho}}$ m/s	$\sqrt{E \cdot \rho}$ Ns/m <sup>3</sup>
Light alloy 70 75 T6	2800	$7.5 \cdot 10^{10}$	5175.4	$1.45 \cdot 10^7$
Steel CroMo	7800	$2.1 \cdot 10^{11}$	5188.7	$4.047 \cdot 10^7$
Titanium 6AL4V	4700	$1.1 \cdot 10^{11}$	4837.8	$2.27 \cdot 10^7$
CFRP UD T300	1650	$1.3 \cdot 10^{11}$	8876.2	$1.464 \cdot 10^7$

#### *2.4 Comments on the Shock Environment Definitions per Shock Response Spectra (SRS) Concept*

It is common practice to define transient excitations by a shock response spectrum (SRS), calculated with SDOF systems having a standard (say  $Q = 10$ ) viscous damping. The shock response spectrum gives the maximum response for each resonant frequency of a potential equipment experiencing the base motion excitation to be specified. This approach (SRS) could be a useful approximation tool if the shock is not too violent ('violent' i.e. 'very high' amplitude for 'very short' duration) although even in these cases, the SRS cancels and/or distorts some important informations.

We believe, however, that pyrotechnic shocks — which are really 'very violent' — need a more precise definition, as this necessity can be proven by the investigations described in this paper.

The specifications of pyrotechnic shocks if based on shock response spectra, belonging to a given damping value (mostly  $Q = 10$ ) should therefore be revised. Indeed, the defined straight lines envelope is not representative even for the tested structure for many reasons:

- i) it does not consider phase relations and multi DOF generalization
- ii) the same shock spectra can belong to an infinite number of excitation time-histories
- iii) shock spectra are not complete without the knowledge of the place and direction of the measurement (or prediction)
- iv) the enveloping of the response curve ignores the feedback effects of the components, and in this way can lead to important over- or under-estimations
- v) the establishment of the shock-spectra should consider the different types of shocks (short duration or long lasting shocks: force/motion/velocity or acceleration shocks, etc.) and their time-histories. Indeed,

e.g. the structural damping can be useful or unimportant or even harmful and decisive according to the type and duration of the shock as well as type and location of the damping.

### 3. Some Representative, Specific Problems in the Aerospace Structure Dynamics

#### 3.1 The Pyrotechnic Separation of the ARIANE 5. 2nd Stage (EPS)

The actual task was the protection of thrusters for the ARIANE 5 attitude control system against pyrotechnic stage separation shocks.

*Fig. 4* shows the configuration of ARIANE 5 with

- main stage
- solid propellant booster EAP
- separation plane

and above separation in a concentric arrangement  
vehicle equipment bay VEB at the periphery  
second stage EPS in central position.

The attitude control thrusters are located at the VEB. They are combined in clusters of three. The clusters are located at the lower edge of the VEB, in order to provide maximum lever arms for the attitude control maneuvers. Thus they are very close to the separation plane.

The local cross-section to be separated by pyrotechnics is an aluminum cylinder with a 5.4 m diameter, 6 mm thick in the separated section.

The shock environment at cluster location was specified in terms of a shock response spectrum (SRS) with a maximum level of 35000 g above 3000 Hz (corresponding to a velocity  $v = 18.6$  m/s), and with amplification factor  $Q = 10$  of the responding 1 DOF system (see *Fig. 5*). This specification corresponds to actual measurements made in a pre-test, where half sine-like shocks with peaks up to 45000 g and a duration up to 80  $\mu$ s have been monitored.

These values are far above the strength of the elements of the mono-propellant thrusters with flow control valves, transducers, catalyst and wire mesh sieves as potentially critical items. Therefore, the design approach was to use shock mounts between 5.4 m cylinder and cluster.

Shock Mounts with *minimum damping* have been found to be efficient against pyrotechnic shocks. The mechanism can be explained by simple idealization as given in *Fig. 5*.

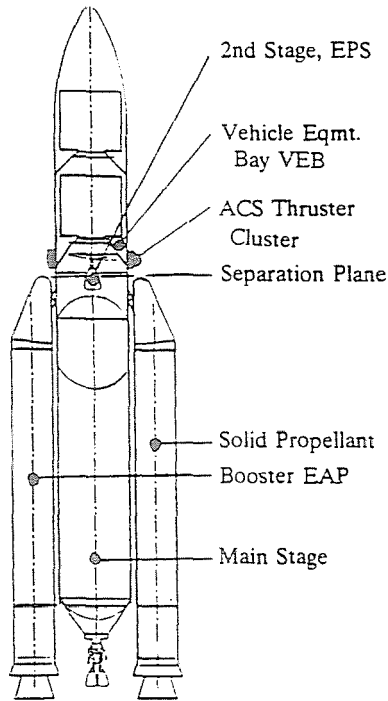


Fig. 4. ARIANE 5 configuration

The excited equipment is idealized as a single degree of freedom (SDOF) system, tuned to a low resonant frequency.

The low damping of the shock mount is represented by the dashpot with a small damping coefficient  $c$ . The shock input is idealized as base motion excitation. Two phases are distinguished which may be typical for a pyroshock environment at a location close to the pyro change:

- First a single pulse with extreme high acceleration level and extreme short duration ( $\tau$ )
- Followed by quasi-cyclic excitation on a much lower level and with much longer duration at high frequencies.

It is understood that no residual displacement and velocity of the base exist after the shock. The response of the SDOF system to the first short duration pulse is mainly due to the forces transmitted by the dashpot, since the duration is too short (i.e.  $f_0\tau \ll 1$ ) to build up relevant relative displacement and spring force. Therefore, the response will be low as long as the damping constant  $c$  is small.

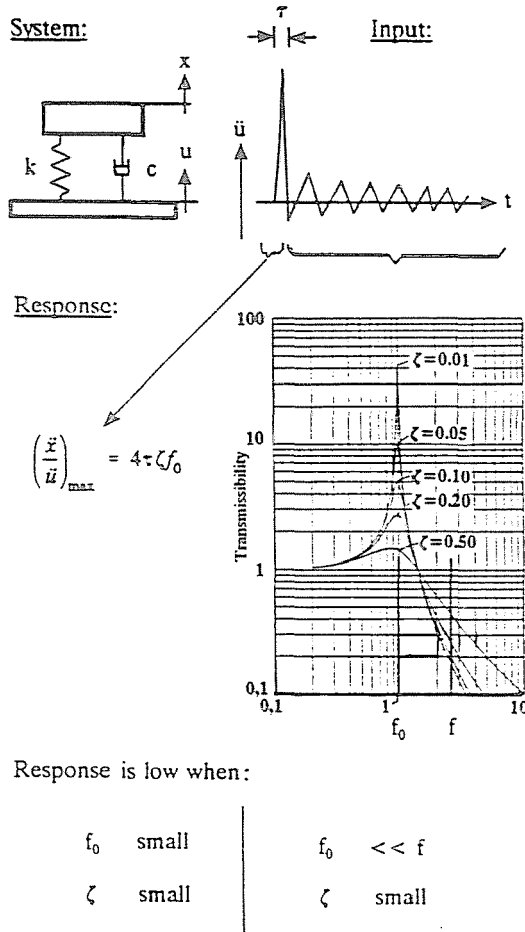


Fig. 5. Shock mount with minimum damping

The response of the SDOF system to the subsequent quasi-cyclic excitation is that to an overcritical stationary excitation, i.e. the responses will be low with the low damping ratio  $\zeta = c/C_{crit}$ .

For extreme *short* shock pulses and for subsequent quasi-cyclic excitation, which is *overcritical*, a shock mount with low damping is advantageous.

**Table 7**  
Acceleration shock with no final displacement

For $0 < t < \tau$	For $t < 0$ and $t > \tau$
$\ddot{u} = a \sin \Omega t$	$\ddot{u} = \dot{u} = u = 0$
$\dot{u} = -\frac{a}{\Omega} \cos \Omega t + A$	
$u = -\frac{a}{\Omega^2} \sin \Omega t + At + B$	
with $A = B = 0$	
but $\dot{u}_{max} = \pm \frac{a}{\Omega}$	
at $t = 0$ and $t = \tau$	
$\Omega = \frac{\pi}{\tau}$	

The second observation was that in the case of a pyro shock, the displacement of the base at the end of the shock event is and remains zero (Table 7).

For short duration shocks, i.e.  $\tau f_0 \ll 1$  provided the system is undamped, only the impulse

$$I = \int \ddot{u} dt$$

is important, not the time-history. If the system is additionally damped, also the initial velocity  $u(t = 0)$  can play a considerable role — especially for extreme short durations.

*Undamped System*

During the time of the shock  $0 < t < \tau$ , the acceleration is due to the spring force

$$\left. \begin{aligned} \ddot{x} &\cong \frac{u_0 k}{m} = \ddot{u}_0 \frac{\omega_0^2}{\Omega^2}; \\ \text{with } \Omega &= \frac{\pi}{\tau}; \quad \omega_0 = f_0 \cdot 2\pi \end{aligned} \right\} \rightarrow \left( \frac{\ddot{x}}{\ddot{u}} \right)_{max} = 4(f_0 \tau)^2 \quad (13)$$

in the initial phase.

After the shock  $t > \tau$ , the system performs a residual vibration

$$\dot{x} = \frac{\int P dt}{m} = \frac{m \ddot{u} \tau \frac{2}{\pi}}{m} \quad \text{and} \quad \ddot{x} = \dot{x} \cdot \omega_0 \quad (14)$$

leading to

$$\left( \frac{\ddot{x}}{\ddot{u}} \right)_{max} = 16 (f_0 \tau)^3 \quad (15)$$

in the residual phase.

*Damped System*

The first observation  $\tau f_0 \ll 1$  allows to neglect the spring force and to concentrate on the damping force.

$$\begin{aligned} F(\text{damp}) &= \dot{u} \cdot c & \text{at } t = 0, \\ \dot{u}c > F(\text{damp}) > -\dot{u}c & & \text{at } 0 < t < \tau. \end{aligned} \quad (16)$$

The second observation;  $u(\text{final}) = 0$ ; allows to define the velocity of the base

$$\dot{u}_{max} = -\frac{a}{\Omega} \quad (17)$$

at  $t = 0$ .

*Eqs.* (16) and (17) yield the max, force within the dashpot at  $t = 0$ .

The resulting acceleration response  $\ddot{x}_{max}$  is:

$$F_{max} = \dot{u}_{max} \cdot c = \frac{1}{\pi} \cdot \ddot{u}_{max} \tau \cdot \zeta \cdot c_{cr}.$$

with

$$c_{cr} = 2\omega_0 m = 4\pi f_0 m,$$

$$F_{max} = 4\ddot{u}_{max} \tau \zeta \cdot f_0 m, \quad (18)$$

$$\ddot{x}_{max} = \frac{F_{max}}{m} = 4\ddot{u}_{max} \tau f_0 \zeta \implies \left( \frac{\ddot{x}}{\ddot{u}} \right)_{max} = 4\tau f_0 \zeta. \quad (19)$$

*Eqs.* (13), (15) and (19) give the shock response evaluations as shown in principle in *Fig. 6*.

*Example:*

$$\ddot{u}_{max} = 40000 \text{ g}$$

$$\tau = 40 \mu\text{s}$$

$$f_0 = 50 \text{ Hz}$$

$$\zeta = 5\%$$

$$\ddot{x}_{max} = 4 \cdot 40000 \cdot 40 \cdot 10^{-6} \cdot 50 \cdot 0.05$$

$$\ddot{x}_{max} = \underline{16} \text{ g} < 0.57f = 28.5 \text{ g (goal)}$$

*Specific Requirements for the Design of Shock Mounts*

With the dimensionless acceleration response

$$\frac{\ddot{x}_{max}}{\ddot{u}_{max}} = 4\tau f_0 \zeta, \quad (20)$$

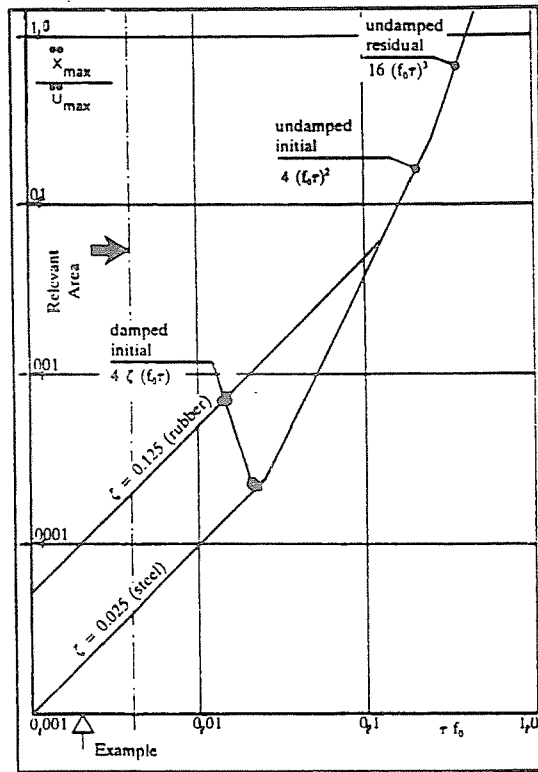


Fig. 6. Response of SDOF system to short duration half-sine pulse

the requirement is to design for

- low resonant frequency  $f_0$ , and
- low damping ratio  $\zeta$ .

Note:

The physical meaning of the above two requirements is to design for a low damping coefficient  $c$ .

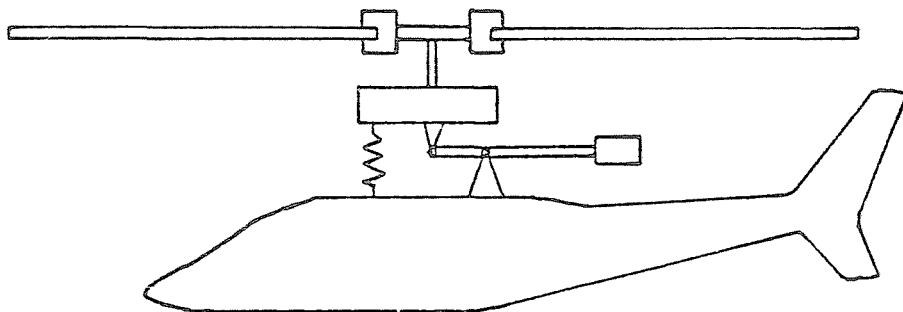
$$c = c_{cr} \cdot \frac{c}{c_{cr}} = 2\omega_0 m \cdot \frac{c}{c_{cr}} = 4\pi f_0 m \zeta .$$

### 3.2 The Helicopter Vibration Isolator

The Helicopter Vibration Isolator (HVI) is an often used device to isolate the periodic rotor excitation from the cabin. As the rotor rotates at a quasi

constant rate — provided the HVI is absolutely undamped — this device completely isolates the rest of the aircraft (*Fig. 7*). But even if a small damping is still present, the reduction of the noise level is considerable at the design frequency and remains also important in a broad frequency range, especially below the design frequency.

$$\begin{array}{r}
 \begin{array}{cc}
 x_2 & x_3 \\
 \hline
 1 - \frac{\omega^2}{\omega_{23}^2} - \frac{\omega^2}{\omega_{523}^2} \left(1 - \frac{l}{a}\right)^2 & -1 + \frac{\omega^2}{\omega_{523}^2} \frac{l}{a} \left(\frac{l}{a} - 1\right) \\
 \hline
 +ig_{23} & -g_{23} \\
 \hline
 -1 + \frac{\omega^2}{\omega_{523}^2} \frac{l}{a} \left(\frac{l}{a} - 1\right) & 1 - \frac{\omega^2}{\omega_{23}^2} - \frac{\omega^2}{\omega_{523}^2} \left(\frac{l}{a}\right)^2 \\
 \hline
 -g_{23} & +ig_{23}
 \end{array} & = 0 \\
 & \\
 & \begin{array}{l}
 \omega_{23}^2 = \frac{k_{23}}{m_2} \\
 \omega_{33}^2 = \frac{k_{23}}{m_3} \\
 \omega_{523}^2 = \frac{k_{23}}{m_5} \\
 k_{02} \sim 0
 \end{array} \\
 \hline
 \end{array} \tag{21}$$



DAVI (Kaman) , IRIS (Boeing-Vertol)

*Fig. 7.* The Helicopter Vibration Isolator (HVI)

It can be seen that if coefficient  $A_{12}$  of the above system of linear equations is zero, amplitude  $x_2$  is zero. This condition is fulfilled if

$$g_{23} = 0$$

and

$$\left(\frac{l}{a}\right)^2 - \left(\frac{l}{a}\right) = k_{23} \frac{1}{m_5 \omega_f^2} . \tag{22}$$

The efficiency of the isolator is shown in a specific case at the tuning frequency and below in *Fig. 8*.



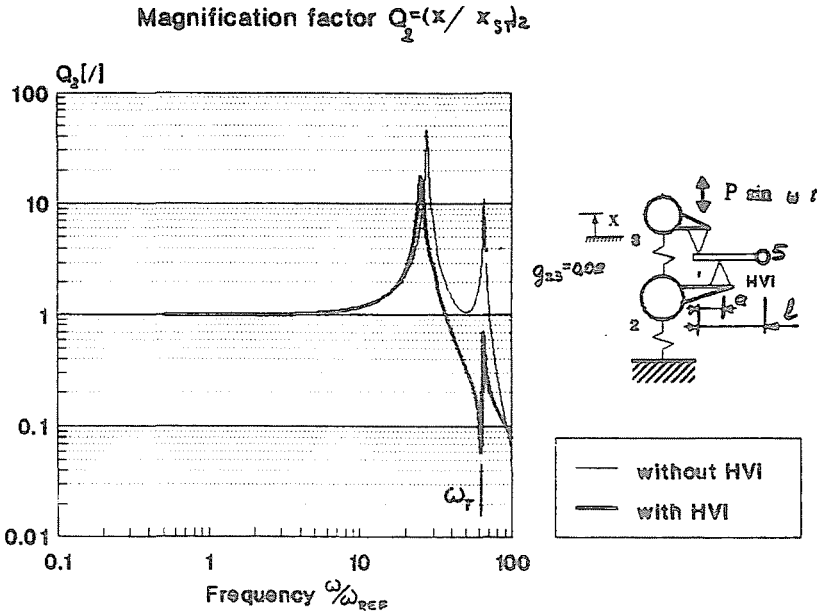


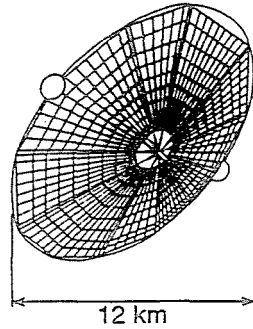
Fig. 8. The efficiency of the isolator in a specific case at the tuning frequency and below

### 3.3 Simplified Dynamic Analyses on Large Imperfect Space Structures

Large space structures which have eigenfrequencies in the order of  $10^{-3}$  to  $10^{-4}$  [Hz], undergo dynamic excitations which can be periodic (e.g. at the orbiting frequency) or shock-like, as sudden load application (crossing the earth shadow) and e.g. control system thruster pulses.

The calculated dynamic response can essentially deviate from that yielded from linear analyses. Indeed, the overall eigenfrequency of a truss-like structure can decrease by some orders of magnitude due to the inevitable imperfection of the struts, and for larger vibration amplitudes a strong non-linearity occurs. Slenderness ratios less than 50 are relatively insensitive against initial crookednesses, they lead, however, to complicated and expensive structures due to the large number of nodal points (Fig. 11). With increasing length and slenderness ratios, the imperfection sensitivity grows and the eigenfrequency of the struts itself decreases.

In this chapter, we will try to evaluate the fundamental influences by means of simple analytical and numerical investigations, and find some indications towards the design of an improved conception.



Three-axis stabilized "wheel"  
with reinforcing spokes

Fig. 9. Examples for large space structures having a surface area of  $100 \text{ km}^2$

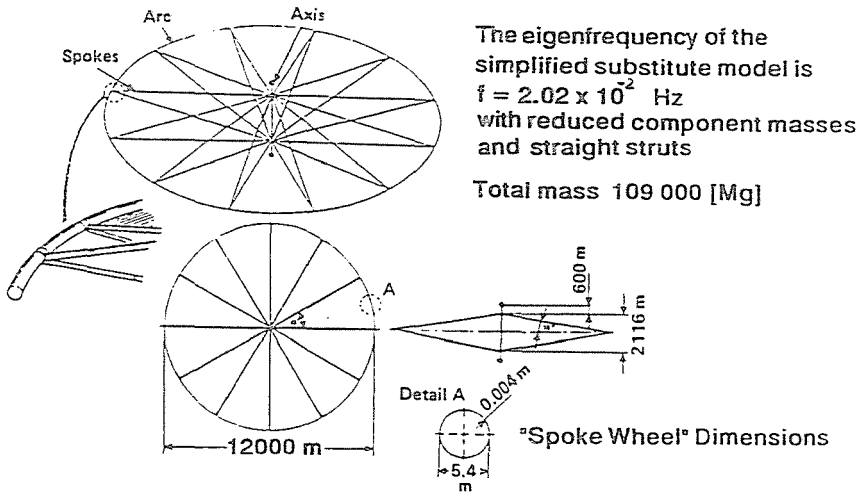


Fig. 10. The 'Spoke Wheel' structural conception

For the first decades of the next century, large space structures up to a surface area of  $100 \text{ km}^2$  are envisaged. They are needed for projects like

- i) solar power plants (photovoltaic or solar dynamic)
- ii) antennas
- iii) platform for mirrors, fabrication, habitation

The main framework for such objects will be a large truss structure which should be transported to the orbit by a large number of launches. In order to reduce the material and transport costs, trusses built-up from

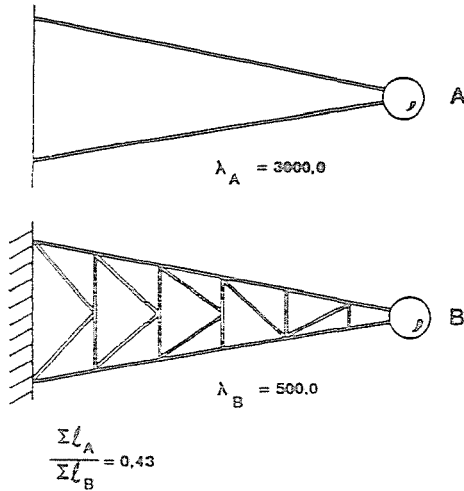


Fig. 11. The comparison of the strut lengths needed for the same truss structure built up of elements having different slenderness ratio

very slender struts having a small number of nodal points will be necessary. As comparison, using the same tubular struts in Fig. 11, version A with a slenderness ratio 3000 needs only 43% of the total length of struts necessary to build version B, where the slenderness ratios are in the order of 500. The large flexible struts of huge space structures are not as straight as desirable. Imperfections, initial curvatures, deflections are unavoidable. Fabrication and assembly tolerances, in principle, can be adjusted by extra-vehicular activities. Thermal and elastic deformations, however, cannot be avoided.

In order to obtain a basic idea on the dynamic behaviour of large truss structures built-up of 'very slender' struts, the following simplifying assumptions will be used for the truss elements:

1. the trusses are simply supported, slender bending beams
2. the structural material is linear-elastic
3. beam bending theory with small/moderate deflections will be used
4. for the beam bending, only one degree of freedom will be considered: a half sine-wave in the plane of the truss
5. the initial imperfection is similar to the assumed bending degree of freedom (see above 4).

Deviations from these assumptions would lead to large non-linear mathematical models which cannot be used for parametric investigations.

**The deformation of an imperfect  
strut under longitudinal load**

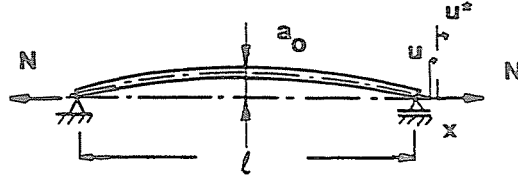


Fig. 12. The influence of imperfection on the stiffness

Let us consider the effective longitudinal stiffness of a strut with a small initial imperfection with amplitude  $a_0$  (Fig. 12) and the shape of a half sine-wave.

The axial elongation of the strut under a tension force  $N$  and a sinusoidal imperfection with amplitude  $a_0$  is:

$$u^* = \frac{Nl}{FE} - \frac{\pi^2}{4} \left( \frac{a}{l} \right)^2 l; \quad \text{with } a = \frac{a_0}{1 + \frac{N}{N_{cr}}}. \quad (23)$$

We find the effective extensional stiffness by derivation

$$\frac{\partial u^*}{\partial N} = \frac{\partial u}{\partial N} = \frac{1}{FE} \left[ 1 + \frac{1}{2} \cdot \frac{a_0^2 F}{2J} \left( 1 + \frac{N}{N_{cr}} \right)^{-3} \right] \quad (24)$$

and the initial value for  $N = 0$  is:

$$\left( \frac{\partial u}{\partial N} \right)_{N=0} / \frac{1}{FE} = 1 + \frac{1}{2} \cdot \frac{a_0^2 F}{J} = 1 + \frac{1}{2} \left( \frac{a_0}{l} \right)^2 \left( \frac{l}{i} \right)^2 \quad (25)$$

herein are

$$i = \sqrt{\frac{I}{E}} \quad \text{and} \quad \lambda = \frac{l}{i} \quad \text{the slenderness ratio.}$$

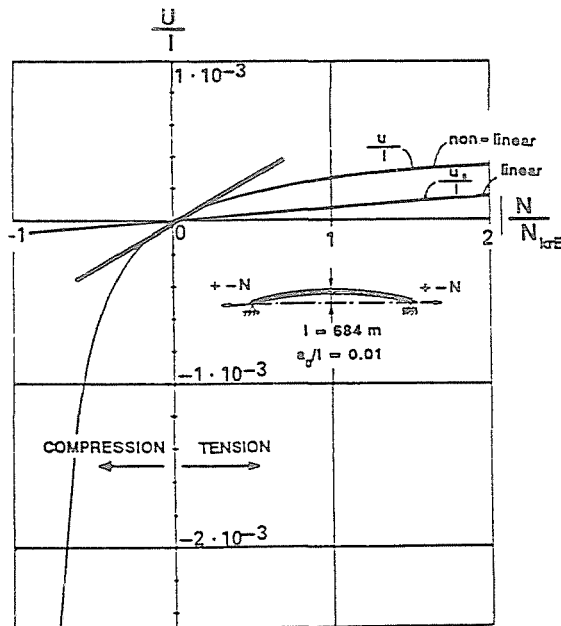
Table 8 shows a comparison of the initial extensional stiffnesses at different imperfections.

In Fig. 15, the mathematical models for further calculations are presented.

The mass of the two struts (in both cases uniformly distributed) is different, the 'above' strut being covered by the solar cell blankets.

**Table 8**  
Comparison of the initial extensional stiffnesses at different imperfections

$\lambda$	$\left(\frac{E_0}{E_{c/f}}\right)_{N=0}$ for		
	$\frac{a_0}{l} = 0.005$	$\frac{a_0}{l} = 0.01$	$\frac{a_0}{l} = 0.05$
Reference			
80	1.08	1.32	9.0
500	3.125	12.5	312.5
3191.2	128.3	510.2	12730.5



The elongation of imperfect struts will be got by integration:

$$\frac{u}{l} = \frac{N}{FE} \left[ 1 + \frac{1}{2} \frac{a_0^2}{l^2} \frac{l^2}{r^2} \frac{2 + \frac{N}{N_{cr}}}{\left(1 + \frac{N}{N_{cr}}\right)^2} \right]$$

Fig. 13. The non-linear elongation of an imperfect column

Model C is a 'V' strut with massless struts, we will analyse the response of this to harmonic excitations.

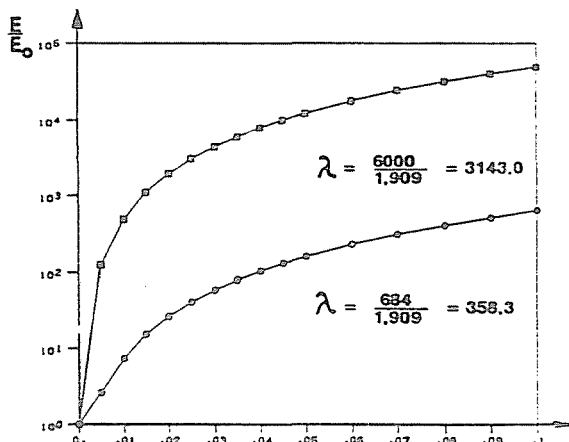
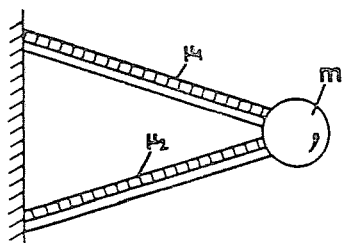


Fig. 14. The relative stiffness vs. imperfection at  $N = 0$



Model	[kg] m	[kg] $\mu_1 l$	[kg] $\mu_2 l$	$m_{\text{res}}$
C	$3,14 \cdot 10^6$	o	o	$3,14 \cdot 10^6$
$D_1$	$3,49 \cdot 10^6$	$1,745 \cdot 10^6$	$1,2 \cdot 10^6$	↑
$D_2$	$2,617 \cdot 10^6$	$2,61 \cdot 10^6$	$1,2 \cdot 10^6$	$6,43 \cdot 10^6$
$D_3$	$0,8723 \cdot 10^6$	$4,36 \cdot 10^6$	$1,2 \cdot 10^6$	↓

Fig. 15. The mathematical models of the 'V-Struts' used in response calculations

The simplest relations will now be shown for model *C* (Fig. 15), i.e. for massless struts, as shown in Fig. 17, where also the expected stiffness curves have been estimated.

In case of harmonic excitations (as occurs by traversing the shadow phase of the orbit), it can be expected — according to these stiffness curves — that

- with straight (perfect) struts, a linear elastic behaviour and classical transmissibility will be found
- with imperfect struts but at 'low excitation levels', the linearized system will lead once more to a linear transmissibility curve, however, with an essentially lower resonance frequency
- with imperfect struts and 'higher' excitation levels, corresponding to the 'softening' non-linear stiffness, the transmissibility will 'turn to

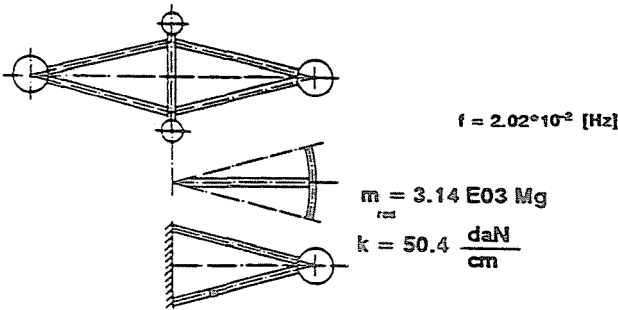


Fig. 16. Reduced system of the spoke wheel configuration

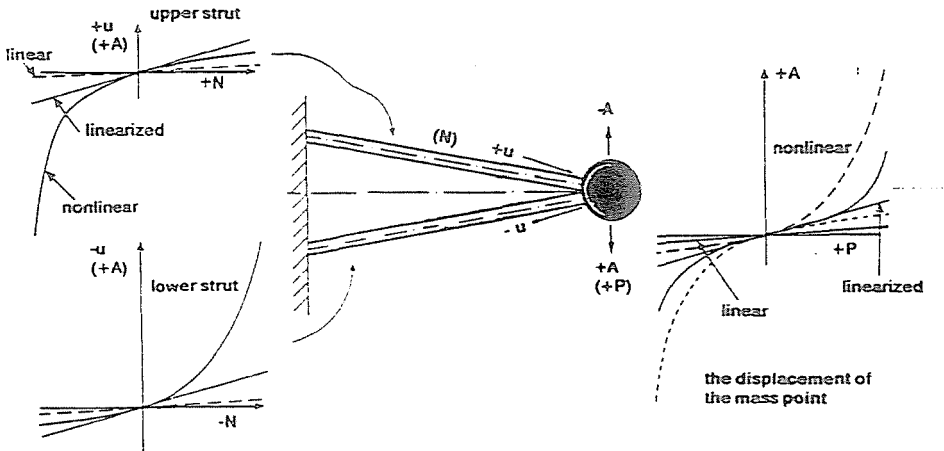


Fig. 17. The definition of the forces and deformations of a 'V-Strut' with a heavy mass and massless struts

left', the higher the response amplitude is, the lower the frequency will be.

Fig. 18 now shows the transmissibility curves for the mathematical model C (Fig. 15), i.e. massless struts for a given excitation level, in one case ( $C_0$ ) without, in the other one with imperfection (1%) designed with ( $C_1$ ). The linear ( $C_0$ ) system has a circular resonance frequency which is

$$\frac{\omega_0}{\omega_1} = \frac{1.26 \cdot 10^{-1}}{5.65 \cdot 10^{-3}} = 22.3 \text{ times}$$

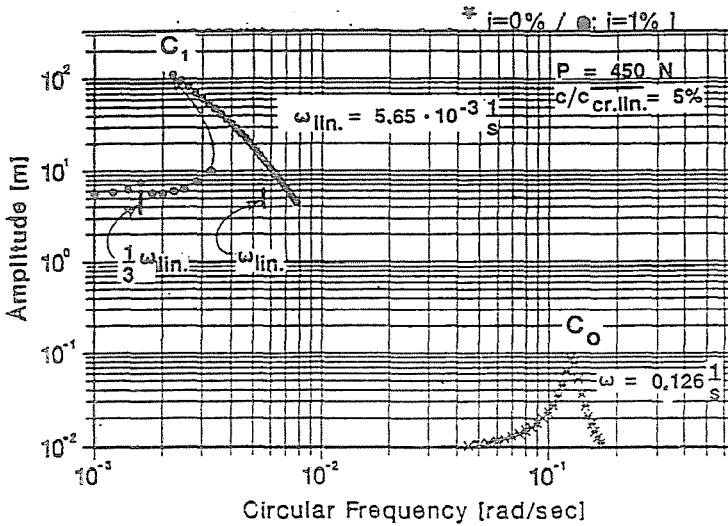


Fig. 18. The transmissibility of a 'V-Strut' with and without imperfection for model 'C'

higher than the linearized frequency of the imperfect system ( $C_1$ ). With the same *relative* damping of 0.05, the relation of the maximum response amplitudes is higher by three orders of magnitude.

The non-linear system shows — as expected — a subcritical resonance at  $(1/3)$  times the linearized resonance frequency.

#### 4. Conclusions

It is desirable that structural engineers working in different fields often exchange their experiences. The author working for 43 years in the aerospace industry found beneficial discussions for both parties during encounters with colleagues working in the civil engineering, machinery, piping or pressure vessel fabrication. Several common interests have been found with dynamic problems in the wind-, earth-quake-, bridge-building engineering.

#### References

1. ÖRY, H. — RITTWEGER, A. — HORNING, E. — LUDWIG, H.: Numerical Results of simplified dynamic analyses on large imperfect space structures, *41st Congr. of the Int. Astron. Feder.*, Dresden, GDR, Oct. 6–12, 1990.
2. ÖRY, H. — HORNING, E. — MAAGER, H.: Pyro Shock Mount Investigation for ARIANE 5-components, *43rd Congr. of the Int. Astron. Feder.*, Washington, D.C. Aug. 28 – Sept. 5, 1992.